Magnetism of self-assembled mono- and tetranuclear supramolecular Ni^{2+} complexes

O. Waldmann, J. Hassmann, and P. Müller
Physikalisches Institut III, Universität Erlangen-Nürnberg, D-91058 Erlangen, Germany

D. Volkmer,* U. S. Schubert,† and J.-M. Lehn
ISIS, 4 rue Blaise Pascal, Université Louis Pasteur, F-67000 Strasbourg, France

(Received 7 April 1998)

The magnetization of a novel supramolecular grid structure consisting of four bis(bipyridyl)-pyrimidine ligands and four Ni^{2+} ions and that of the mononuclear analogue $Ni(terpy)_2$ was measured. Magnetic anisotropy was determined from investigations of powder as well as of crystal samples. We provide evidence for an intramolecular antiferromagnetic coupling of the four Ni^{2+} spins of the tetranuclear species with $J=-8$ K. The magnetization of the mononuclear complex is typical for a $S=1$ spin with zero field splitting. The magnetization of the tetranuclear grid is discussed in terms of the effective spin Hamiltonian appropriate for Ni^{2+} ions including various higher order exchange terms. In particular, significant indications for a biquadratic term of about $J'=0.5$ K is found. [S0163-1829(98)05630-6]

Since the discovery of intramolecular magnetic interactions in copper acetate,[1,2] polynuclear complexes have been of considerable interest to both physicists and chemists as they can serve as model systems to investigate exchange interactions. In such systems intermolecular interactions are frequently much smaller than intramolecular interactions, which in principle makes it possible to treat them without resorting to the approximations necessary for materials that have, e.g., collective magnetic interactions.[3,4] The discovery of the HDVV Hamiltonian and crystal-field theory stimulated the development of the effective spin Hamiltonian formalism by Abragam, Pryce, Stevens, and others,[5] which has been proved to be a very successful semiempirical theory to interpret experimental data of polynuclear complexes, as well as other magnetic materials. However, a calculation or even prediction of its parameters from the crystal structure of the complexes still appears to be a difficult task.[4,6,7] Nevertheless, the present theories of superexchange[8] are successful in interpreting various magnetostructural correlations.[4,7] For binuclear complexes, which are the systems investigated most thoroughly in this respect, considerable progress has been achieved in the last three decades.[9,4] In the case of complexes of higher nuclearity, which are of additional interest as they are extended to higher dimensions, the quantitative theory is much less developed.[4,7] This is probably because comparing theoretical with experimental results, it is not always easy to distinguish whether inconsistencies arise due to, e.g., approximations used in the theoretical calculation or because the investigated system does not fulfill all the simplifications assumed in the calculation.

In a recent study, we demonstrated that properly designed self-assembled supramolecular $[2\times2]$-grid structures containing four Co^{2+} ions, denoted as Co-$[2\times2]$, exhibit intramolecular antiferromagnetic coupling of the four Co^{2+} spins.[10] To our knowledge, the $[2\times2]$ grids represent the first experimental realization of a tetranuclear cluster with magnetic centers arranged in a clear and simple square planar fashion. We believe that the $[2\times2]$-grid system is of particular interest as it represents an ideal quantum spin system in the following sense: the topology of the coupling is simple and perfectly square planar and thus rather amenable to theoretical interpretations, a possible intermolecular coupling is quite weak, and finally the coupling strength being of about several K is of the ''right'' order, since on the one hand it is high enough to allow for measurements at temperatures where the experimental results are unaffected by possible intermolecular couplings and on the other hand it is low enough to allow to measure, e.g., magnetization steps with experimentally accessible magnetic fields.

We should point out that the $[2\times2]$ grids also evoke considerable interest as potential molecular building blocks[11] as they allow for a derivation of the ligand end groups making it possible to functionalize the grids with respect to their film properties, their transferability and arrangements on interfaces, etc.[11] For example, recently it has been shown, that ordered thin films and even monolayers of grids can be transferred to various substrates,[12,13] which is an important condition for a potential employment of the grids, e.g., as molecular storage devices.

In this work, we investigated the magnetization of the supramolecular $[2\times2]$-grid structure with four Ni^{2+} metal centers, denoted as Ni-$[2\times2]$, which is isomorphic to Co-$[2\times2]$. We will show that the four Ni^{2+} spins are coupled by intramolecular antiferromagnetic exchange interactions. In order to demonstrate the effects of the antiferromagnetic coupling, we also investigated the magnetization of $Ni(terpy)_2$, the mononuclear analog of the Ni-$[2\times2]$ grids. We present a careful interpretation of the data in terms of the spin Hamiltonian formalism in order to establish convincingly which of the various well-known possible exchange terms are necessary to describe the magnetic behavior of Ni-$[2\times2]$.

So far, the crystal structure of the Ni-$[2\times2]$ grids has not been determined, so we refer to the crystal structure of the isomorphic Co-$[2\times2]$ grids.[14] It consists of four bis(bipyridyl)-pyrimidine ligands[15] and four metal centers (Fig. 1), in our case Ni^{2+} ions. Each metal center is situated in the crossing point of two ligands and is enclosed by six N

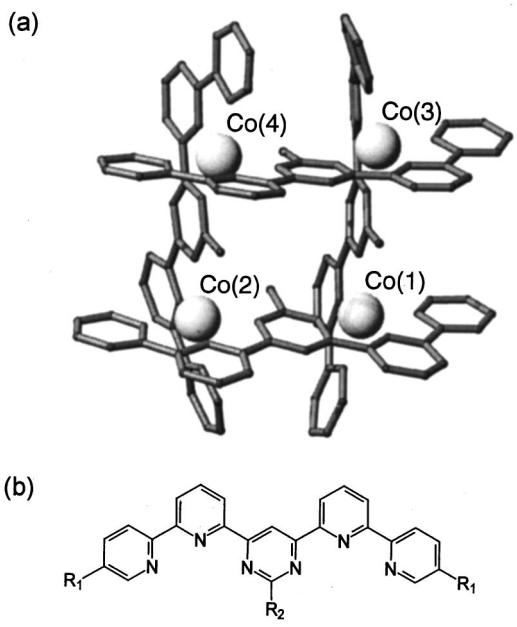

FIG. 1. (a) Crystal structure of the Co-[2×2] grid. (b) Bis(bipyridyl)-pyrimidine ligand with R_1=H and R_2=CH_3.

donor atoms in an almost octahedral geometry. In the Co grid, the distance between the metal centers is about 6.47 Å. The average bond length from the N donors to the metal centers is 2.14 Å. The octahedron of the six N atoms surrounding each metal center exhibits a considerable tetragonal compression with a small orthorhombic distortion. The corresponding bond lengths are about 2.03, 2.16, and 2.23 Å. The positive charges are countered by eight PF_6^- ions. The grids were formed by self-assembly in methanol and investigated in acetonitrile (CH_3CN) solution.[14,16] Crystals were prepared by diffusion of methanol into a concentrated acetonitril solution in a closed atmosphere yielding light brown rhombic crystals. The crystal axes were denoted with a,b,c in order to distinguish them from the molecular or magnetic axes, respectively, denoted by x,y,z. It is evident from the shape of the crystals that the c axis and z axis coincide. Powder samples were prepared by air drying the crystals.

We also performed measurements on the mononuclear analog of the Ni-[2×2] grids, the Ni(terpyridyl)$_2$(PF_6)$_2$ complex, denoted here as Ni-[1×1]. This is the obvious system for comparison as the Ni^{2+} ions have the same chemical environment and coordination to the ligands, but are not magnetically coupled. For synthesis, a method analogous to that for the Ni-[2×2] grids was used.[16] The crystal structure reveals a tetragonally compressed octahedral arrangement of the six N atoms[17] due to the stereochemical demands of the ligand.[18] The Ni-$N_{central}$ bond length is 2.02 Å and the Ni-N_{distal} bond length 2.14 Å. Using the method described in Ref. 16, orthorhombic crystals were obtained. The crystallographic axes and the magnetic axes, respectively, should coincide with the crystal edges.

The temperature and magnetic field dependence of the magnetic moment $m(T,B)$ was measured with a commercial superconducting quantum interference device magnetometer (Quantum Design). The temperature range was 1.9–250 K and the maximum field 5.5 T. The powder and crystal samples were fixed with apiezon grease on a plastic straw. The background signal of the plastic straw was found to be below the resolution of the magnetometer.

For the powder samples the background signal of the grease was corrected for in the following way. First the magnetization of a drop of grease put on the straw was measured at 250 K and 1 T. From that, the magnetization of the grease in the whole temperature and field range could be extrapolated with an accuracy of 5%. Then the powder was fixed in the grease. The signal of the grease was typically 30% of that of the sample at 250 K, but could be corrected for with an accuracy of 2.5%. At lower temperatures the accuracy of this correction improves as the magnetization of the sample increases. The weight of the powder samples was typically 2.5 mg and could be measured with an accuracy of about 50 μg.

The Ni-[1×1] crystal could be fixed with a very small amount of grease so that the signal of the grease was negligible. The edges of the crystal could be aligned with an accuracy of ±5° parallel to the magnetic field. Magnetization was measured for all three directions. The crystal weight was 3.64 mg.

In the case of the Ni-[2×2] crystals, first one crystal was selected by light microscopy. As the Ni- [2×2] crystals are transparent, imperfections could be easily detected and we believe that the chosen crystals were of excellent quality. Then, it was necessary to put the crystal directly from the solution into grease and to cover it carefully with the grease, otherwise the crystal would have decomposed within few seconds. Therefore the sealing with grease was essential and a considerable background signal from the grease was unavoidable. Its level has been estimated to be about 10–20% of the signal of the sample at 250 K, but a more accurate determination was not possible. Therefore the data were not corrected for it. The crystal embedded in grease was then mounted on the straw and cooled down rapidly to 50 K. At these temperatures the crystals were stable for at least several days. After being measured, the crystal was crushed to powder directly on the straw and measured again. In this way the contribution of the grease to the magnetization remained equal for both measurements and the small anisotropy of the magnetization typical for Ni^{2+} ions could be investigated reliably. In several cases the crystal could be rotated without breaking to a second orientation before being crushed. Finally, the weight of the powder and grease mixture was measured. Following this procedure, five crystals were investigated. The weight of the crystals was typically 20 μg. The c axis and the ab plane of the crystals were aligned with an accuracy of ±5° parallel to the magnetic field. The a and b axes could not be distinguished.

The diamagnetic contribution of the ligands was determined from measurements of Cd-[2×2] and Cd(terpy)$_2$(PF_6)$_2$. For both complexes we obtained $\chi_D = -0.6(\pm 0.1)\times 10^{-3}$ μ_B/(spin T) in fair agreement with an estimation using Pascal's constants. However, we did not correct the data for it. Instead, the temperature-independent contribution was determined from the magnetization at high temperatures.

In this work we use μ_B/spin, the number of Bohr magnetons per metal ion, as unit for the magnetic moment. For the [2×2] grids, 1 μ_B/spin corresponds to 22 340 cm^3 G mol^{-1} and for the [1×1] complexes, 1 μ_B/spin corresponds to 5585 cm^3 G mol^{-1}. In the case of the powder

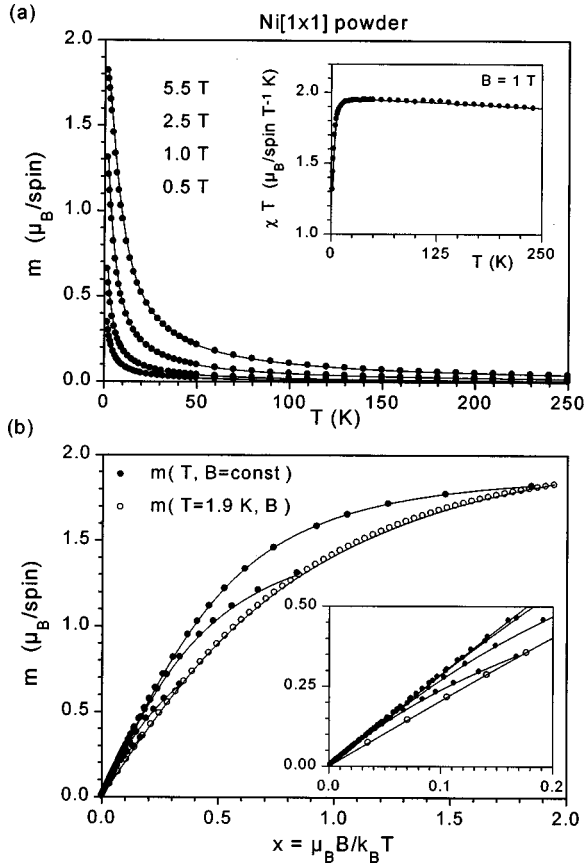

FIG. 2. (a) Temperature dependence of the magnetic moment of Ni-[1×1] powder. Magnetic fields were 0.5, 1, 2.5, and 5.5 T from bottom to top. The inset shows χT obtained from the magnetic moments at 1 T. (b) Magnetic moment of Ni-[1×1] powder vs the reduced variable $x=\mu_B B/k_B T$. The same data being presented in panel (a) is indicated by closed circles. The result of a field sweep measurement at 1.9 K is assigned by open circles. In both panels, solid lines represent a fit to the data using the Hamiltonian Eq. (1) (see text).

and Ni-[1×1] crystal samples, the number of metal ions was calculated from the measured weight and the molecular weight of the complexes including metal ions, ligands, and counter ions. For the powder samples these values might be several percent too low due to residual solvent and water. The Ni-[2×2] crystal measurements have been calibrated by comparing the magnetic moment of the crushed crystals with that of the powder samples at 50 K.

In Fig. 2(a) we present the temperature dependence of the magnetic moment for Ni-[1×1] powder measured at several magnetic fields. In Fig. 2(b) the same data together with the results of a field sweep measurement at 1.9 K is plotted as function of $x=\mu_B B/k_B T$. Here, k_B denotes the Boltzmann constant. Above 50 K the temperature dependence is well described by $\chi T=C+\chi_0 T$ [see inset of Fig. 2(a)], where $\chi=m/B$ and $C=1.97\,\mu_B/\text{spin T}^{-1}\,\text{K}$, $\chi_0=-0.3\times10^{-3}\mu_B/(\text{spin T})$. Taking into account the diamagnetic contribution of the ligands, a temperature-independent susceptibility of about $0.3\times10^{-3}\mu_B/(\text{spin T})$ is left which we attribute to an incomplete correction of the grease. From the Curie constant C the g factor and the effective magnetic moment are determined to be $g=2.1$ and $\mu_{\text{eff}}=2.97$. For $Ni(terpy)_2Br_2$, Hogg and Wilkins[19] obtained $\mu_{\text{eff}}=3.1$ at 293 and 77 K, Judge and Baker[20] obtained $\mu_{\text{eff}}=3.09$ at 250 K and $\mu_{\text{eff}}=3.00$ at 150 K, in reasonable agreement with our result. At lower temperatures a clear deviation from the Curie law was observed [inset of Fig. 2(a)]. This is attributed, as usual, to the presence of a zero-field-splitting (ZFS). The Ni-[1×1] system can be described by the well-known effective spin Hamiltonian[21–23]

$$H=D(S_z^2-\tfrac{2}{3})+E(S_x^2-S_y^2)+\mu_B g_\alpha B_\alpha S_\alpha-\tfrac{1}{2}\chi_0 B^2, \quad (1)$$

with $S=1$. D, E are the ZFS parameters, g_α are the g factors, and χ_0 is the temperature-independent susceptibility. In the following, $\alpha,\beta=x,y,z$ and summation over repeated indices is applied. Using conventional least square fitting algorithms, we obtained $D=-8.775$ K, $E=0.168$ K, and $g=2.095$, where χ_0 was held constant. The calculated curves using these parameters are shown as solid lines in Fig. 2, demonstrating the quality of the fit in the whole temperature and magnetic field regime. However, similar results were obtained with slightly different parameters being about $D=-9$ K, $E\approx0$ K, and $g=2.1$.

In view of the tetragonally compressed octahedron of nitrogen atoms surrounding the Ni^{2+} ion, $D>0$ should be expected from ligand field theory,[21,24] in contrast to the experimental result. The reason for this discrepancy is unclear. All attempts to reproduce the experimental results with $D>0$ were unsuccessful. Henke and Reinen[25] performed ESR measurements on $Ni(terpy)_2Br_2$. As they did not observe a signal even for 35 GHz and 4.2 K, they concluded, in view of the geometrical arrangement of the nitrogen atoms, that $D>4.5$ K. However, with the magnetic field configuration $B\perp B_{\text{rf}}$ usually used in ESR experiments, a $\Delta M=2$ transition is forbidden[21,26] and we suppose that the result of Henke and Reinen is also consistent with $D<-4.5$ K.

In order to confirm our result of the powder measurements, we investigated a Ni-[1×1] crystal. Figure 3(a) shows the temperature dependence of χT for several magnetic fields applied in two different directions. The data for the third direction has been omitted for clarity. The axis of highest anisotropy has been denoted with z. Figure 3(b) presents the field dependencies of the magnetic moment for all three field directions at $T=1.9$ K. Figure 3(b) immediately demonstrates that the ZFS parameter D has to be negative since m_z clearly exhibits a first order magnetic moment, and that E has to be almost zero since m_x and m_y are almost equal. Here, m_z means $m(B\|z)$ and analogous for m_x and m_y. In Fig. 3 calculated curves for $D=-9$ K, $E=0$, $g=2.15$, and $\chi_0=0$ are also shown as solid lines. The g factor is slightly larger than that obtained for the powder samples. The agreement of calculated and experimental curves is not as good as in the case of the powder. However, it should be noted that the discrepancies are not due to an incorrectly chosen D or E. Otherwise, the maxima seen in the upper two m_z curves of Fig. 3(a) and the field dependencies of m_x and m_y, respectively, shown in Fig. 3(b) would not be reproduced. Instead, the discrepancies arise because the absolute values of the magnetic moment do not match. This might be explained by the following two arguments.

(1) At higher temperatures the calculated values for m_z are lower than the experimental ones, while those for $m_{x(y)}$ are higher. Here, $m_{x(y)}$ is used to refer to m_x or m_y. This

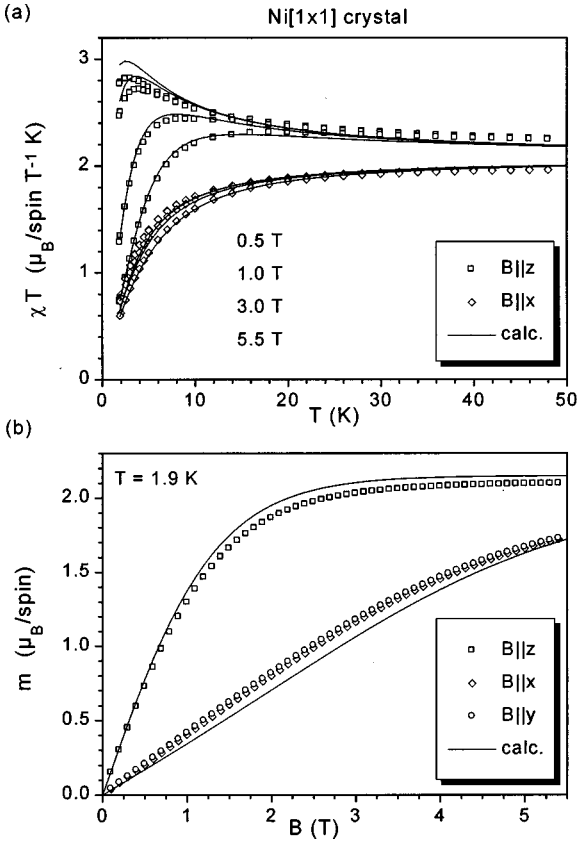

FIG. 3. (a) Temperature dependence of χT of a Ni-[1×1] crystal with the magnetic field parallel to the *z* axis (open squares) and to the *x* axis (open diamonds). Magnetic fields were 0.5, 1, 3, and 5.5T from top to bottom for each field direction. (b) Magnetic field dependence of the magnetic moment of a Ni-[1×1] crystal at 1.9 K with the magnetic field parallel to the *z* axis (open squares), to the *x* axis (open diamonds), and to the *y* axis (open circles). In both panels, solid lines represent a calculation using the Hamiltonian Eq. (1) (see text). Parameters were $D=-9$ K, $E=0$, $g=2.15$, and $\chi_0=0$.

suggests an anisotropy of the g factor, such that $g_z>g_{x(y)}$. Indeed, this is expected if $D<0$ as is seen from the well-known effective spin Hamiltonian derived for a singlet orbital ground state[21,22]

$$H=-\lambda^2\Lambda_{\alpha\beta}S_\alpha S_\beta+\mu_B(2\delta_{\alpha\beta}-\lambda\Lambda_{\alpha\beta})B_\alpha S_\beta, \qquad (2)$$

where λ is the spin orbit coupling constant and $\Lambda_{\alpha\beta}$ is a tensor determined by the properties of the ligand field.[22] In the principal axis system this Hamiltonian can be written as

$$H=AS(S+1)+D[S_z^2-\tfrac{1}{3}S(S+1)]+E(S_x^2-S_y^2)+\mu_B g_\alpha B_\alpha S_\alpha. \qquad (3)$$

It is clear that since $\Lambda_{\alpha\beta}$ enters in the ZFS parameters as well as in the g factors, relations between both exist. That is, the g factors can be expressed in terms of A, D, and E (and λ). In particular, restricting ourselves to tetragonal symmetry for simplicity one obtains the equation

$$g_z-g_{xy}=2D/\lambda, \qquad (4)$$

where the meaning of g_{xy} is obvious. As $\lambda<0$ for Ni^{2+},[21] $g_z>g_{xy}$ demands for $D<0$ and vice versa. The experimental observation that $g_z>g_{x(y)}$ thus further confirms that indeed $D<0$. In view of the fact that ligand field theory suggests a wrong sign for D as discussed above, it might be argued that Eq. (4) also does. However, this is not true as the ligand field enters in the above equations only via $\Lambda_{\alpha\beta}$. In some sense, the interplay between ZFS parameters and g factors is mainly determined by the orbital part of the wave functions and is correctly reproduced by Eq. (2). In contrast, the actual splitting pattern of the energy levels (which determines the sign of *D)* calculated from the geometrical arrangement of the ligands is highly sensitive to the radial part of the wave functions.[24] From the magnetic moments at 50 K the anisotropy of the g factor has been estimated to $g_z/g_{xy}=1.025$ and, using $g=2.15$, $g_z-g_{xy}=0.05$. Equation (4) then yields a surprisingly reasonable value for the spin orbit coupling constant $\lambda=-250\ \mathrm{cm}^{-1}$.[24] The ligand field splitting parameter Dq was found to be 1250 cm^{-1} for both $Ni(terpy)_2Br_2$ (Ref. 25) and $Ni(terpy)_2(ClO_4)_2$.[18] The g factor calculated from $g=2-8\lambda/10Dq$ (Ref. 21) is $g=2.16$, in fair agreement with our result.

(2) At lower temperatures the relationships are inverted. Now the calculated values for m_z are higher while those for $m_{x(y)}$ are lower than the experimental ones, indicating that either the magnetic fields were not aligned perfectly parallel to the principal axes or, most likely, that the crystal investigated was not absolutely perfect. It is clear that the reduction of m_z and the enhancement of $m_{x(y)}$, respectively, will be more pronounced the higher the ratio $m_z/m_{x(y)}$ is. In Fig. 3(a) it is seen that at lower temperatures the calculated curves for 5.5 T fit the experimental data significantly better than at lower fields. Indeed, at, e.g., 0.5 T the ratio $m_z/m_{x(y)}$ is about 3.25, while at 5.5 T it is only 1.2 [see Fig. 3(b)], supporting the above suggestion. At higher temperatures $m_z/m_{x(y)}$ is again close to 1. It has been explained above that the deviations in this regime arise because the anisotropy of the g factor was neglected in the calculation. But the discussion in this paragraph indicates that the above estimation of the g factor anisotropy might be too small.

For Ni-[2×2] powder, the temperature dependence of the magnetic moment measured at several magnetic fields is presented in Fig. 4(a). The same data converted to χT is shown in Fig. 4(b). The inset of Fig. 4(b) depicts the magnetic field dependence at 1.9 K. In contrast to Ni-[1×1], the temperature dependence of the magnetic moment of Ni-[2×2] reveals a maximum at ≈13 K indicating an antiferromagnetic coupling of the four Ni^{2+} ions within a grid. Indeed, the calculated curves according to the isotropic exchange Hamiltonian[6]

$$H_{\mathrm{ex}}=H_{\mathrm{AF}}+\sum_{i=1}^{4}(\mu_B g_\alpha B_\alpha S_{i\alpha}-\tfrac{1}{2}\chi_0 B^2), \qquad (5)$$

$$H_{\mathrm{AF}}=-J(\mathbf{S}_1\cdot\mathbf{S}_2+\mathbf{S}_2\cdot\mathbf{S}_3+\mathbf{S}_3\cdot\mathbf{S}_4+\mathbf{S}_4\cdot\mathbf{S}_1), \qquad (6)$$

with $J=-8$ K, $g=2.05$, and $\chi_0=-0.3\times10^{-3}\mu_B/$(spin T), reproduce the data well. This is demonstrated in Fig. 4. Only at the lowest temperatures significant deviations occur, as is most clearly seen in the inset of Fig. 4(b), and much of the following discussion will deal with the origin of

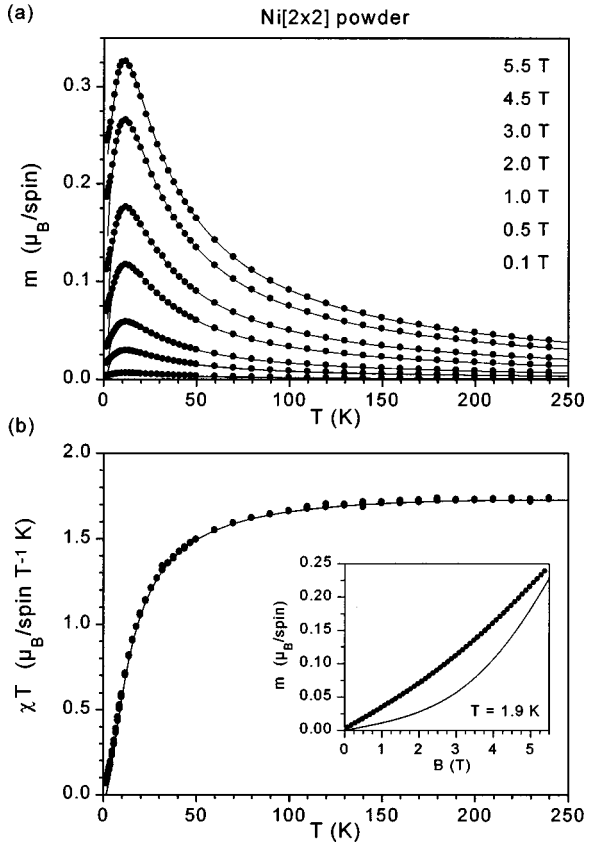

FIG. 4. (a) Temperature dependence of the magnetic moment of Ni-[2×2] powder. Magnetic fields were 0.1, 0.5, 1, 2, 3, 4.5, and 5.5 T from bottom to top. (b) Temperature dependence of χT of Ni-[2×2] powder for the same fields as in panel (a). The inset shows the magnetic field dependence of the magnetic moment at 1.9 K. In both panels, solid lines represent a calculation using the Hamiltonian H_{ex} (see text). Parameters were $J=-8$ K, $g=2.05$, and $\chi_0=-0.3\times10^{-3}\mu_B$/(spin T).

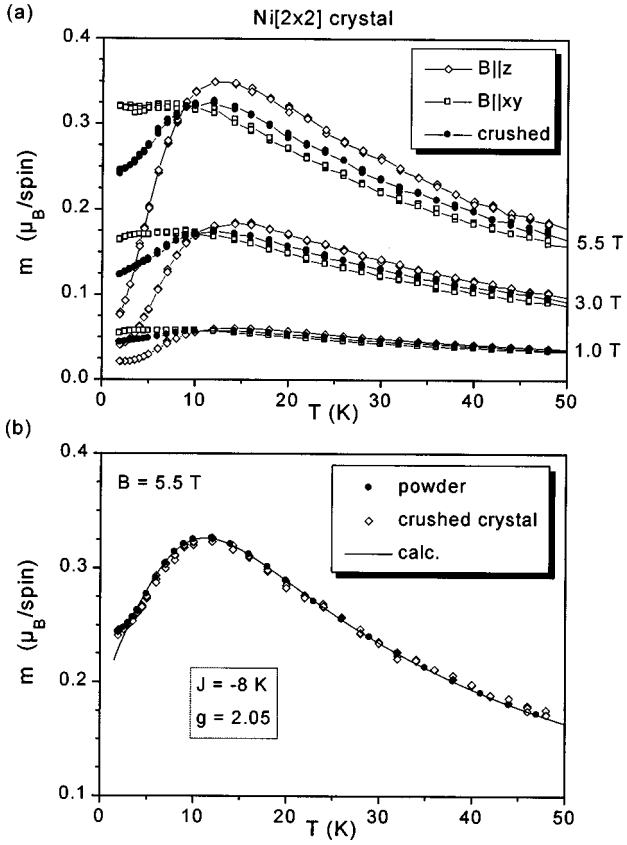

FIG. 5. (a) Temperature dependence of the magnetic moment of Ni-[2×2] crystals with the magnetic field parallel to the z axis (open diamonds) and to the xy plane (open squares), respectively, and for crushed crystals (solid circles). Magnetic fields were 1, 3, and 5.5 T from bottom to top. Lines are guides to the eye. (b) Comparison of the temperature dependence of the magnetic moments at 5.5 T for powder samples (closed circles) and crystal samples (open diamonds) of Ni-[2×2]. The solid line represents a calculation using the Hamiltonian H_{ex} (see text). Parameters were $J=-8$ K, $g=2.05$, and $\chi_0=-0.3\times10^{-3}\mu_B$/(spin T).

this discrepancy. The obtained g factor is significantly to small, but this is attributed to a possible overestimation of the number of metal ions in the samples.

Figure 5(a) presents the temperature dependence of the magnetic moment of Ni-[2×2] crystals, exhibiting a clear anisotropy of the magnetic moment for fields applied parallel to the c axis of the crystal and perpendicular to it. Within experimental error no anisotropy in the ab plane was observed. As for the case of Ni-[1×1] the axis of highest anisotropy has been assigned with z and the corresponding magnetic moment with m_z. The magnetic moment for fields perpendicular to the c axis will be denoted by m_{xy} and that of the crushed crystals by $\langle m\rangle$. The three curves for m_z, m_{xy}, and $\langle m\rangle$ cross each other in one point at ≈10 K. This fact provides further support that any anisotropy in the ab plane must be very small, since with $\langle\chi\rangle=\frac{1}{3}(\chi_x+\chi_y+\chi_z)$ and $\chi_{xy}=\cos^2(\phi)\chi_x+\sin^2(\phi)\chi_y$ it is easily seen that $\langle\chi\rangle=\chi_z=\chi_{xy}$ is equivalent to $\chi_x=\chi_y$. Here ϕ denotes the experimentally unknown angle of the magnetic field in the ab plane. Figure 5(b) demonstrates the good agreement of the measurements of the crushed crystals and the powder samples. For comparison, the calculated curve according to Eqs. (5) and (6) is also depicted. The above-mentioned deviation from data below 5 K is evident. In view of the anisotropy and this deviation it is obvious that the isotropic exchange Hamiltonian needs to be supplemented.

In the following we will consider several contributions: a single ion anisotropy expressed in terms of a ZFS and a g factor anisotropy, a very weak amount of impurities possibly present, a next-nearest-neighbor coupling, and the various exchange terms derived for coupled ions with a singlet orbital ground state, i.e., anisotropy exchange, antisymmetric exchange, and biquadratic exchange.[21,6] The importance of each term was investigated using the following procedure. First, the susceptibility $\chi(T)$ obtained from the powder measurements at 0.5 T was fit to the average susceptibility calculated numerically from the corresponding Hamiltonian using standard least square fitting algorithms. Then, the magnetic moments $m_z(T,B)$, $m_{xy}(T,B)$, and $\langle m(T,B)\rangle$ were calculated for all fields using the obtained parameters and compared with the crystal measurements. For clarity we only present the curves at a field of 5.5 T. A comparison of experimental and calculated curves at this field, at which the magnetization already clearly deviates from linearity [see inset of Fig. 4(b)], is more advantageous than a comparison of

the susceptibilities, as this allows us to not only check the temperature dependence but also the correct magnetic field dependence. The temperature independent susceptibility χ_0 was always set to $\chi_0 = -0.3\times10^{-3}\mu_B/(\text{spin T})$. If a g-factor anisotropy was allowed for, g_{xy} and g_z were determined such that the average g factor $\langle g\rangle = [\frac{1}{3}(2g_{xy}^2+g_z^2)]^{(-1/2)}$ remained equal to 2.05. χ_0 and the g factors were held constant during the fitting procedure. In order to test the significance of our results we took into account an additional contribution to the magnetic moment due to impurities. We assumed $g=2.1$ and $S=1$, appropriate for Ni^{2+}. The impurity density was parametrized by the molar fraction ϱ. The results were as follows.

(1) *Single ion anisotropy*. The results on Ni-[1×1] strongly suggest the presence of a ZFS in Ni-[2×2] as well. Indeed, a g-factor anisotropy alone cannot reproduce the crystal data, especially the crossing point at ≈10 K. The various exchange terms are known to be small[6] and are thus hardly believed to explain the anisotropy. Thus, the terms describing a ZFS definitely need to be added to H_{ex}. From the similarity of the geometrical arrangement of the N atoms in both Ni-[1×1] and Ni-[2×2], it is expected that D should also be negative for Ni-[2×2]. Indeed, $D<0$ can be directly inferred from the fact that at higher temperatures $m_z > m_{xy}$ holds [Fig. 5(a)]. Using the high-temperature expansion for the susceptibility of Eq. (1) to second order in $1/T$, the condition $\chi_z > \chi_{xy}$ can be rewritten as $g_z^2(1-\frac{1}{3}D/k_BT) > g_{xy}^2(1+\frac{1}{6}D/k_BT)$.[21,27] Taking into account Eq. (4), it follows that $\chi_z > \chi_{xy}$ is equivalent to $D<0$. This argument still holds in the presence of exchange couplings. Concerning the ZFS parameter E, the experimental results might allow for a small *ab* anisotropy, but E should not exceed ≈1 K. In our calculations we found that such a small E had almost no influence on the magnetization in the experimentally accessible range, while larger E worsened the agreement between data and calculation. Therefore E can be safely neglected. Thus, the ZFS adds a term[6]

$$H_{\text{ZFS}} = \sum_{i=1}^{4} [D(S_{iz})^2 - \tfrac{2}{3}] \tag{7}$$

to the Hamiltonian Eq. (5). The result of a least square fit for the Hamiltonian $H = H_{\text{ex}} + H_{\text{ZFS}}$ is depicted in Fig. 6(a). The g factor was taken to be isotropic, i.e., $g_z = g_{xy}$, and impurities were neglected, i.e., $\varrho = 0$. The obtained parameters were $J = -7.55$ K and $D = -10.70$ K. The experimental data is not perfectly reproduced, but the temperature dependence of the calculated curves resembles that of the experimental ones. Especially, the typical curvature of m_{xy} and $\langle m\rangle$ below 5 K is obtained which was not described by the isotropic exchange Hamiltonian H_{ex} [Fig. 5(b)]. This curvature will be important in the following, because if it is not reproduced by theory then this indicates that the magnetic field dependence is not correctly described. At ≈50 K the calculated curves are less spread than the measured curves, indicating a g-factor anisotropy of the form $g_z > g_{xy}$, which in fact is expected from Eq. (4). Thus, we tried to refine the fit by setting $g_z - g_{xy} = 0.08$ and allowing for impurities. The result is depicted in Fig. 6(b). The parameters were found to be $J = -8.24$ K, $D = -6.21$ K, and $\varrho = 0.344\%$. The data are now

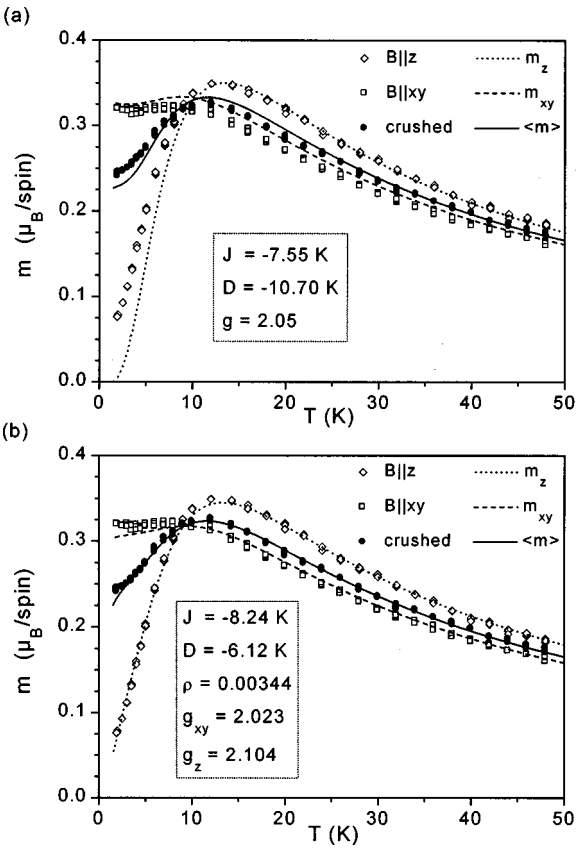

FIG. 6. Temperature dependence of the magnetic moment of Ni-[2×2] crystals with magnetic field parallel to the z axis (open diamonds) and to the xy plane (open squares), respectively, and for crushed crystals (solid circles). Lines represent fits using the Hamiltonian $H_{\text{ex}} + H_{\text{ZFS}}$ (see text). Parameters are given in the panels and $\chi_0 = -0.3\times10^{-3}\mu_B/(\text{spin T})$.

excellently described for temperatures above 5 K. However, the typical curvature below 5 K is no longer reproduced. This was found generally if impurities were allowed for. An impurity density of $\varrho \approx 0.35\%$ is reasonable. A refinement considering only the g-factor anisotropy did not lead to an improvement, although the calculated values for m_{xy} of course shifted to lower values. However, at the lowest temperatures, the calculated values for m_z still remained almost zero so that the deviation of the theoretical calculated curve for $\langle m\rangle$ and the crushed crystal data actually increased.

(2) *Next-nearest-neighbor exchange.* To our knowledge, a next-nearest-neighbor interaction has not been observed so far to be relevant in interpreting the magnetization of clusters. Nevertheless, for completeness we considered this term, which in our case is written as

$$H_{\text{NN}} = -J_{\text{NN}}(\mathbf{S}_1\cdot\mathbf{S}_3 + \mathbf{S}_2\cdot\mathbf{S}_4). \tag{8}$$

We also could not find any indication of its importance, since including H_{NN} in our calculations did not result in any significant improvements.

(3) *Anisotropic exchange.* This exchange adds a term

$$H_A = D_J S_{iz}\cdot S_{jz} - \tfrac{1}{3}\mathbf{S}_i\cdot\mathbf{S}_j \tag{9}$$

to the Hamiltonian.[6] Here, summation over $(i,j) = (1,2),(2,3),(3,4),(4,1)$ is applied. Due to the large dis-

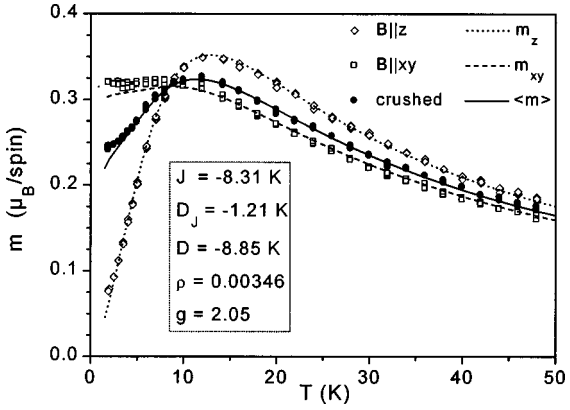

FIG. 7. Temperature dependence of the magnetic moment of Ni-[2×2] crystals with magnetic field parallel to the z axis (open diamonds) and to the xy plane (open squares), respectively, and for crushed crystals (solid circles). Lines represent a fit using the Hamiltonian $H_{\mathrm{ex}}+H_{\mathrm{ZFS}}+H_A$ (see text). Parameters are given in the panel and $\chi_0=-0.3\times10^{-3}\mu_B/(\mathrm{spin\ T})$.

tance of 6.5 Å between the Ni^{2+} ions, a contribution of the magnetic dipolar interaction[6] to the anisotropic coupling can be neglected. Thus, the anisotropic coupling is of orbital nature and its magnitude has been estimated to $D_J\propto(\Delta g/g)^2J$.[6,28,29] However, it has been pointed out that this estimation might also be completely wrong.[6] Fitting the powder susceptibility to the Hamiltonian $H=H_{\mathrm{ex}}+H_{\mathrm{ZFS}}+H_A$ with an isotropic g factor and impurities neglected, led to unreasonably high values for D_J. More seriously, $m_z<m_{xy}$ was found in the whole temperature regime, in complete disagreement with the experimental observation. However, allowing for the presence of impurities but still taking an isotropic g factor, a reasonable fit could be obtained, as shown in Fig. 7. We obtained $J=-8.31$ K, $D_J=-1.21$ K, $D=-8.85$ K, and $\varrho=0.346\%$. The agreement with data is quite good, but the following objections have to be made. First, the specific curvature below 5 K is not reproduced. Second, the ZFS parameter D clearly demands for a g-factor anisotropy [see Eq. (4)]. However, with, e.g., $g_z-g_{xy}=0.05$ the agreement is considerably worsened. Finally, in view of the above estimate, the magnitude of D_J seems to be somewhat too high.

(4) *Antisymmetric exchange.* This exchange term is of the form[28,29]

$$\mathbf{K}_{ij}\cdot(\mathbf{S}_i\times\mathbf{S}_j), \tag{10}$$

with the same summation convention as before. However, $\mathbf{K}_{ij}$ is identical to zero if the paramagnetic centers are related by a symmetry element.[6,29,30] Indeed, the symmetry of the [2×2] grid is approximately C_{2v}, requiring $\mathbf{K}_{ij}=0$.

(5) *Biquadratic exchange.* Beyond the bilinear terms considered above, the biquadratic term is the most important higher-order term. It is of the form[6]

$$H'=J'(\mathbf{S}_i\cdot\mathbf{S}_j)^2 \tag{11}$$

with the same summation convention applied as above. The magnitude of J' is generally believed to be of the order of $10^{-2}J$.[6,31] Nevertheless, in magnetization and ESR experiments it often has been found that biquadratic terms should

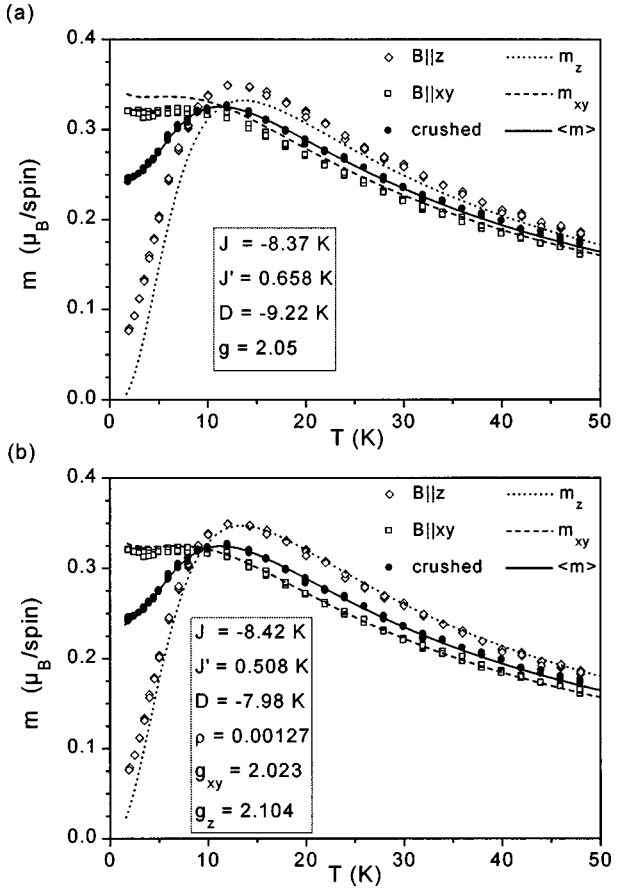

FIG. 8. Temperature dependence of the magnetic moment of Ni-[2×2] crystals with magnetic field parallel to the z axis (open diamonds) and to the xy plane (open squares), respectively, and for crushed crystals (solid circles). Lines represent fits using the Hamiltonian $H_{\mathrm{ex}}+H_{\mathrm{ZFS}}+H'$ (see text). Parameters are given in the panel and $\chi_0=-0.3\times10^{-3}\mu_B/(\mathrm{spin\ T})$.

be taken into account.[26,3] In fact, the Hamiltonian $H=H_{\mathrm{ex}}+H_{\mathrm{ZFS}}+H'$ led to the best fits of the powder susceptibility, irrespective of whether g-factor anisotropy and/or impurities were included or not. The curves for $J=-8.37$ K, $J'=0.658$ K, and $D=-9.22$ K with an isotropic g factor and with impurities neglected are presented in Fig. 8(a). The excellent agreement between powder or crushed crystal measurements, and calculated values is evident. m_z and m_{xy} are not reproduced as well, but the deviations are mainly due to the neglected g-factor anisotropy, indicated by the lower spread of the calculated curves at ≈50 K. The best fit was obtained by including g-factor anisotropy and impurities, as demonstrated in Fig. 8(b). The parameters were $J=-8.42$ K, $J'=0.508$ K, $D=-7.98$ K, and $\varrho=0.127\%$. For Fig. 8(b), $g_z-g_{xy}=0.08$ has been used, but $g_z-g_{xy}=0.05$ also led to an almost equally good fit. It should be noted that the specific curvature below 5 K is reasonably reproduced. The biquadratic term was found to be the only term which can describe the specific curvature below 5 K even with impurities included. Furthermore, using the Hamiltonian $H=H_{\mathrm{ex}}+H_{\mathrm{ZFS}}+H'+H_A$ led to $D_J=0$, demonstrating that biquadratic exchange is more important than anisotropic exchange. The only objection concerning the biquadratic term which can be made is that the absolute value of J' seems to be somewhat too high. Uryû and Friedberg[32] showed that a

biquadratic term is not the most general quadrulinear exchange term. They considered the case of three coupled spins, and obtained an additional term

$$[(\mathbf{S}_1\cdot\mathbf{S}_2)(\mathbf{S}_2\cdot\mathbf{S}_3)+(\mathbf{S}_2\cdot\mathbf{S}_3)(\mathbf{S}_3\cdot\mathbf{S}_1)+(\mathbf{S}_3\cdot\mathbf{S}_1)(\mathbf{S}_1\cdot\mathbf{S}_2)] \tag{12}$$

which they argued to be more important than the biquadratic term. To our knowledge, their considerations have not been extended to the case of four spins in a square planar arrangement. In view of Eq. (12) we tentatively assumed

$$H''=J''[(\mathbf{S}_1\cdot\mathbf{S}_2)(\mathbf{S}_2\cdot\mathbf{S}_3)+(\mathbf{S}_2\cdot\mathbf{S}_3)(\mathbf{S}_3\cdot\mathbf{S}_4)+(\mathbf{S}_3\cdot\mathbf{S}_4)\times(\mathbf{S}_4\cdot\mathbf{S}_1)+(\mathbf{S}_4\cdot\mathbf{S}_1)(\mathbf{S}_1\cdot\mathbf{S}_2)]. \tag{13}$$

Using H'' we obtained results quite similar to H', suggesting that other quadrilinear terms than the biquadratic might be actually relevant. However, without a detailed calculation at hand it is not clear whether terms such as, e.g., $(\mathbf{S}_1\cdot\mathbf{S}_2)(\mathbf{S}_3\cdot\mathbf{S}_4)$ need to be included, and it is difficult to assess the significance of our results obtained for H''.

The above discussion of Ni-[2×2] demonstrates that the isotropic interaction is about $J=-8$ K and that the single ion anisotropy plays an important role, expressed by $D\approx-8$ K and $g_z-g_{xy}\approx 0.05\ldots0.08$. Furthermore, there is evidence for a biquadratic exchange on the order of $J'=0.5$ K.

To summarize, we have studied the magnetization of a novel supramolecular grid structure, the Ni-[2×2] grid containing four Ni^{2+} ions in a square-type arrangement. We demonstrated the presence of an intramolecular antiferromagnetic coupling of the four metal centers. Using the effective spin Hamiltonian formalism appropriate for Ni^{2+} ions, we were able to reproduce the measurements for both powder and crystal samples simultaneously. We presented a detailed discussion of the various additionally possible terms which might contribute to the magnetization, i.e., single ion anisotropy, next-nearest-neighbor exchange, anisotropic exchange, antisymmetric exchange, and biquadratic exchange. The most important additional term was found to be the single ion anisotropy, but significant indications for a biquadratic exchange were also obtained. For comparison, powder and crystal samples of the mononuclear Ni(terpy$_2$) complex have been investigated. The results could be reproduced by taking into account a zero field splitting, confirming the single ion anisotropy parameters obtained for the Ni-[2×2] grids. We conclude that the Ni-[2×2] species represents an almost ideal model system to investigate magnetic interactions in a discrete entity. We believe that supramolecular systems with a defined number of magnetic ions are suitable for future investigations, contributing to a deeper insight into molecular magnetic coupling mechanisms, and we hope that this work will stimulate corresponding theoretical work.

The authors wish to thank C. Reimann, W. Junker, and R. Koch for valuable discussions. Partial financial support by the Bayerische Forschungsstiftung via the FORSUPRA consortium, and the Deutsche Forschungsgemeinschaft is gratefully acknowledged. D.V. thanks the Alexander von Humboldt-Stiftung (Germany) and U. S. S. the Stiftung Stipendien-Fonds der Chemischen Industrie e.V. (Germany) for financial support.

*Present address: Fakultät für Chemie, Anorganische Chemie 1, Universität Bielefeld, D-33501 Bielefeld, Germany.

†Present address: Lehrstuhl für Makromolekulare Stoffe, Technische Universität München, D-85747 Garching, Germany.

[1] B. Bleaney, Rev. Mod. Phys. **25**, 161 (1953).

[2] B. Bleaney, F. R. S. Bowers, and K. D. Bowers, Proc. R. Soc. London, Ser. A **214**, 451 (1952).

[3] A. P. Ginsberg, Inorg. Chim. Acta **45**, 817 (1971).

[4] O. Kahn, *Molecular Magnetism* (VCH, New York, 1993).

[5] M. H. L. Pryce, Proc. Phys. Soc. London, Sect. A **63**, 25 (1950); A. Abragamn and M. H. L. Pryce, Proc. R. Soc. London, Ser. A **205**, 135 (1951); K. W. H. Stevens, *ibid.* **65**, 209 (1951).

[6] A. Bencini and D. Gatteschi, *Electron Paramagnetic Resonance of Exchange Coupled Systems* (Springer, Berlin, 1990).

[7] R. D. Willet, D. Gatteschi, and O. Kahn, *Magneto-Structural Correlations in Exchange Coupled Systems* (Reidel, Dordrecht, 1983).

[8] P. W. Anderson, Phys. Rev. **115**, 2 (1959); P. J. Hay, J. C. Thibault, and R. Hoffmann, J. Am. Chem. Soc. **97**, 4884 (1975); K. W. H. Stevens, Phys. Rep. **24**, 1 (1976); O. Kahn and B. Briat, J. Chem. Soc., Faraday Trans. 2 **72**, 268 (1976).

[9] O. Kahn, Angew. Chem. **97**, 837 (1985).

[10] O. Waldmann, J. Hassmann, P. Müller, G. S. Hanan, D. Volkmer, U. S. Schubert, and J.-M. Lehn, Phys. Rev. Lett. **78**, 3390 (1997).

[11] U. S. Schubert, J.-M. Lehn, J. Hassmann, C. Y. Hahn, N. Hallschmid, and P. Müller, in *Functional Polymers*, edited by A. O. Patil, D. N. Schulz, and B. M. Novak (American Chemical Society, Washington, DC, in press).

[12] J. Hassmann, N. Hallschmid, C. Y. Hahn, H.-J. Schleemilch, P. Müller, G. S. Hanan, D. Volkmer, U. S. Schubert, and J.-M. Lehn (unpublished).

[13] G. S. Hanan, U. S. Schubert, D. Volkmer, J.-M. Lehn, J. Hassmann, C. Y. Hahn, O. Waldmann, P. Müller, G. Baum, and D. Fenske, in *9th International Symposium on Molecular Recognition and Inclusion,* edited by A. Colman (Kluver Academic, Dordrecht, in press).

[14] G. S. Hanan, U. S. Schubert, D. Volkmer, E. Riviere, J.-M. Lehn, N. Kyritsakas, and J. Fischer, Can. J. Chem. **75**, 169 (1997); G. S. Hanan, Ph.D. thesis, Université Louis Pasteur, Strasbourg, 1995.

[15] G. S. Hanan, U. S. Schubert, D. Volkmer, J.-M. Lehn, G. Baum, and D. Fenske, Angew. Chem. Int. Ed. Engl. **109**, 1929 (1997).

[16] U. S. Schubert, C. H. Weidl, M. Eigner, C. Eschbaum, and J.-M. Lehn (unpublished).

[17] M. I. Arriortua, T. Rojo, J. M. Amigo, G. Germain, and J. P. Declercq, Bull. Soc. Chim. Belg. **91**, 337 (1982).

[18] A. T. Baker, D. C. Craig, and A. D. Rae, Aust. J. Chem. **48**, 1373 (1995).

[19] R. Hogg and R. G. Wilkins, J. Chem. Soc. **1962**, 341.

[20] J. S. Judge and W. A. Baker, Inorg. Chim. Acta **1**, 68 (1967).

[21] A. Abragam and B. Bleaney, *Electron Paramagnetic Resonance of Transition Ions* (Clarendon, Oxford, 1970).

[22] M. H. L. Pryce, Nuovo Cimento **1**, 817 (1957).

[23] K. W. H. Stevens, Proc. R. Soc. London, Ser. A **214**, 237 (1952).

[24] C. J. Ballhausen, *Introduction to Ligand Field Theory* (McGraw-Hill, New York, 1962).

[25] W. Henke and D. Reinen, Z. Anorg. Allg. Chem. **436**, 187 (1977).
[26] G. E. Pake and T. L. Estle, *The Physical Principles of Electron Paramagnetic Resonance* (Benjamin, London, 1973).
[27] T. Haseda and M. Date, J. Phys. Soc. Jpn. **13**, 175 (1958).
[28] K. W. H. Stevens, Rev. Mod. Phys. **25**, 166 (1953).
[29] T. Moriya, Phys. Rev. **120**, 91 (1960); I. Dzyaloshinsky, J. Phys. Chem. Solids **4**, 241 (1958).
[30] A. Bencini and D. Gatteschi, Mol. Phys. **47**, 161 (1982).
[31] N. L. Huang and R. Orbach, Phys. Rev. Lett. **12**, 275 (1964).
[32] N. Uryû and S. A. Friedberg, Phys. Rev. **140**, 1803 (1965).